MSC2010: 70K50, 65C30, 60H30

© *A. P. Kolinichenko, L. B. Ryashko*

MODALITY ANALYSIS OF PATTERNS IN REACTION-DIFFUSION SYSTEMS WITH RANDOM PERTURBATIONS

In this paper, a distributed Brusselator model with diffusion is investigated. It is well known that this model undergoes both Andronov–Hopf and Turing bifurcations. It is shown that in the parametric zone of diffusion instability the model generates a variety of stable spatially nonhomogeneous structures (patterns). This system exhibits a phenomenon of the multistability with the diversity of stable spatial structures. At the same time, each pattern has its unique parametric range, on which it may be observed. The focus is on analysis of stochastic phenomena of pattern formation and transitions induced by small random perturbations. Stochastic effects are studied by the spatial modality analysis. It is shown that the structures possess different degrees of stochastic sensitivity.

Keywords: reaction-diffusion model, Turing instability, self-organization, pattern formation, noise-induced dynamics, modality analysis.

DOI: 10.20537/2226-3594-2019-53-07

Introduction

The study of self-organization [1, 2] is a challenging task for modern science. One of the many mechanisms is spatial pattern formation caused by diffusion instability, first modeled and studied by Alan Turing in 1952 [3]. Various patterns were discovered in biology, chemistry, physics and other fields of science. With proper mathematical methods, assisted by computer modeling, pattern formation dynamics can be studied and predicted.

A necessary part of the modeling process is the simulation of random perturbations. In fact, these seemingly small interferences are present in every system. Here, the most fundamental example is the Brownian motion in any kind of substance. These perturbations are chaotic and unpredictable, yet often they are the cause for stability and order. Therefore, the study of stochastic phenomena in dynamical systems is crucial for understanding self-organization processes in nature.

The analysis of pattern formation mechanisms attracts researchers from diverse fields of natural science (see [4–8]).

This work is devoted to studying the various phenomena connected with the pattern formation in the distributed Brusselator model with diffusion [9]. Section 1 introduces deterministic pattern formation in the parametric zone of Turing instability. It is shown that the system under consideration is multistable: for the same parameter values various different patterns can be generated, while the form depends on initial conditions. Additionally, most patterns appear in their specific parametric zones. We perform a modality analysis of the transient behavior in the pattern formation.

Section 2 is devoted to noise-induced phenomena in the model with random perturbations. First, the phenomenon of the stochastic pattern generation is considered. It is shown that the perturbed model is able to generate temporarily stable structures similar to the patterns formed in the instability zone. Next, pattern transformations under the influence of small noise are investigated by modality analysis. These transformations show sensitivity difference of pattern types.

§ 1. Diffusion instability and patterns

The stochastic distributed Brusselator model defined by the system of two diffusion equations is considered:

$$\begin{aligned} \frac{\partial u}{\partial t} &= a - (b+1)u + u^2 v + D_u \frac{\partial^2 u}{\partial x^2} + \gamma\xi, \\ \frac{\partial v}{\partial t} &= bu - u^2 v + D_v \frac{\partial^2 v}{\partial x^2} + \gamma\eta. \end{aligned} \tag{1.1}$$

Here, $u(t,x)$, $v(t,x)$ are concentrations of the reagents, parameters a and b are positive, D_u and D_v are diffusion coefficients, $\xi(t,x)$ and $\eta(t,x)$ are two independent random processes, and γ is the noise intensity coefficient. The scalar spatial variable x belongs to the $[0,L]$ interval. The system has the following zero-flux boundary conditions:

$$\frac{\partial u}{\partial x}(t,0) = \frac{\partial u}{\partial x}(t,L) = \frac{\partial v}{\partial x}(t,0) = \frac{\partial v}{\partial x}(t,L) = 0. \tag{1.2}$$

The state of a distributed system, in which the values of system variables are uniform through space and equal to the equilibrium values of the corresponding nondistributed system is called a *homogeneous equilibrium state*. The instability of homogeneous equilibrium in the diffusion system is called *Turing instability* or *diffusion instability*. Loss of stability is called *Turing bifurcation*.

Stable spatially nonhomogeneous states are formed in the parametric zone of Turing instability. In this paper we fix $a = 3$, $D_v = 10$, and $L = 40$. The Andronov–Hopf boundary is $b_{AH} = 10$ and the Turing boundary is $b_T = \left(1 + \sqrt{0.9 D_u}\right)^2$. These borders are shown in Fig. 1.

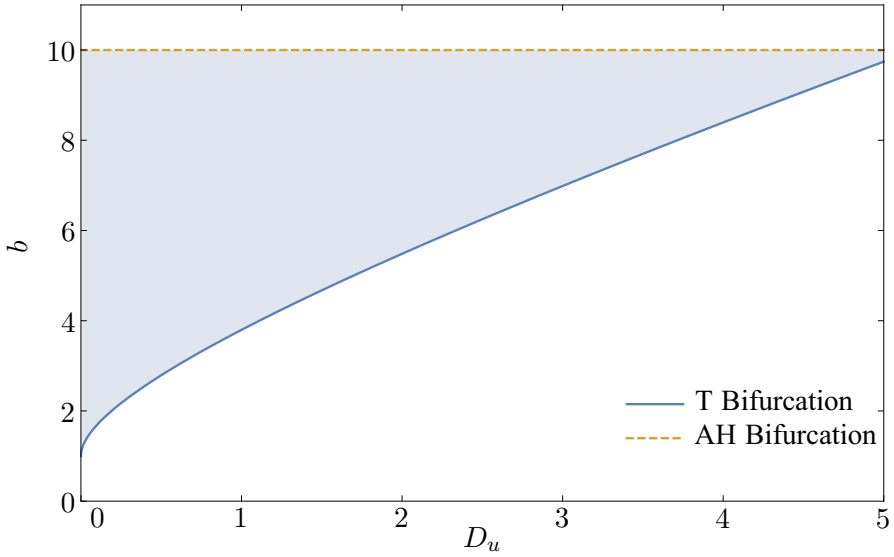

Fig 1. Bifurcation diagram of Brusselator (1.1) with $a = 3$, $D_v = 10$, $\gamma = 0$.

R e m a r k 1.1. Note that bifurcation boundaries can be found analytically. For these evaluations it is assumed that the random perturbations are excluded ($\gamma = 0$).

For numerical modeling of solutions $u_{j,i} = u(t_j, x_i)$, $v_{j,i} = v(t_j, x_i)$ of the system 1.1, we used the following explicit scheme 1.3 with the temporal step τ and the spatial step h:

$$\begin{cases} u_{j+1,i} = u_{j,i} + \tau f_{j,i} + \tau D_u \dfrac{u_{j,i-1} - 2u_{j,i} + u_{j,i+1}}{h^2} + \gamma \xi_{j,i}, \\ v_{j+1,i} = v_{j,i} + \tau g_{j,i} + \tau D_v \dfrac{v_{j,i-1} - 2v_{j,i} + v_{j,i+1}}{h^2} + \gamma \eta_{j,i}, \end{cases} \tag{1.3}$$

where

$$f_{j,i} = f(u_{j,i}, v_{j,i}), \quad g_{j,i} = g(u_{j,i}, v_{j,i}), \quad t_j = j\tau, \quad x_i = ih,$$
$$f(u,v) = a - (b+1)u + u^2 v, \quad g(u,v) = bu - u^2 v,$$
$$\tau = 10^{-4}, \quad h = 0.2.$$

Here, $\xi_{j,i}$ and $\eta_{j,i}$ are uncorrelated Gaussian noises with intensity γ and parameters $E\xi_{j,i} = E\eta_{j,i} = 0$, $E\xi_{j,i}\xi_{k,l} = E\eta_{j,i}\eta_{k,l} = \delta_{j,i}\delta_{k,l}$.

Let $b = 9$, $\gamma = 0$, in this case the Turing bifurcation value is $D_u^* = 4.(4)$. The influence of noise is excluded, making the model entirely deterministic. Initial conditions are generated using the following discrete scheme:

$$u_{0,i} = \bar{u} + \varepsilon \cos\left(\frac{2\pi x_i \lambda}{L}\right), \quad v_{0,i} = \bar{v} + \varepsilon \cos\left(\frac{2\pi x_i \lambda}{L}\right). \tag{1.4}$$

By adjusting parameters ε and λ, various spatial deviations from the homogeneous equilibrium state $\bar{u}, \bar{v}$ can be produced. These periodic forms satisfy the zero-flux boundary conditions (1.2) if λ is an integer or a half-integer and can be used as the initial state in numerical simulations. Changing these conditions yields various stable patterns for fixed values of D_u (see Fig. 2).

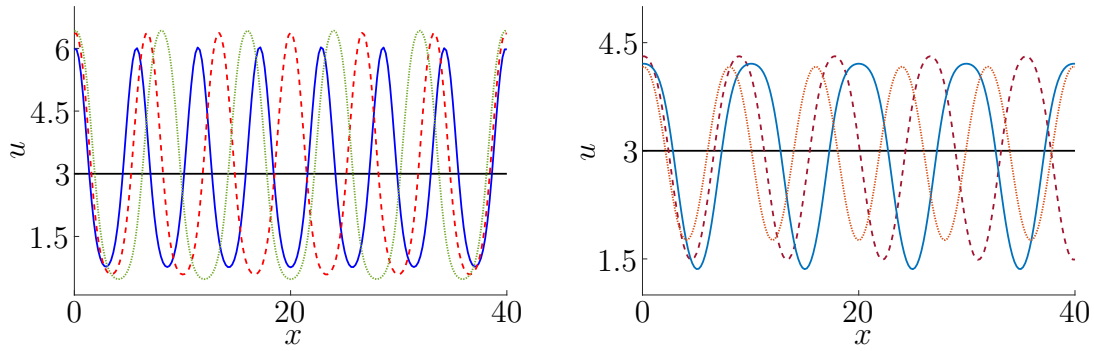

Fig 2. Examples of spatial patterns: $D_u = 2$ (left), $D_u = 4$ (right)

The patterns appear as wave-like structures of varying periodicity and tendency on the left edge of the system space. To distinguish them we use the number of peaks (integer or half-integer) and direction (up or down).

Changing the diffusion coefficient affects the shape of the patterns. In the examples shown in Fig. 3, the 4-peak patterns (left) are generated for $D_u = 2.5$ (solid), $D_u = 3.3$ (dashed) and $D_u = 4.0$ (dotted), and the 4.5-peak patterns (right) are generated for $D_u = 2.0$ (solid), $D_u = 3.0$ (dashed) and $D_u = 4.0$ (dotted).

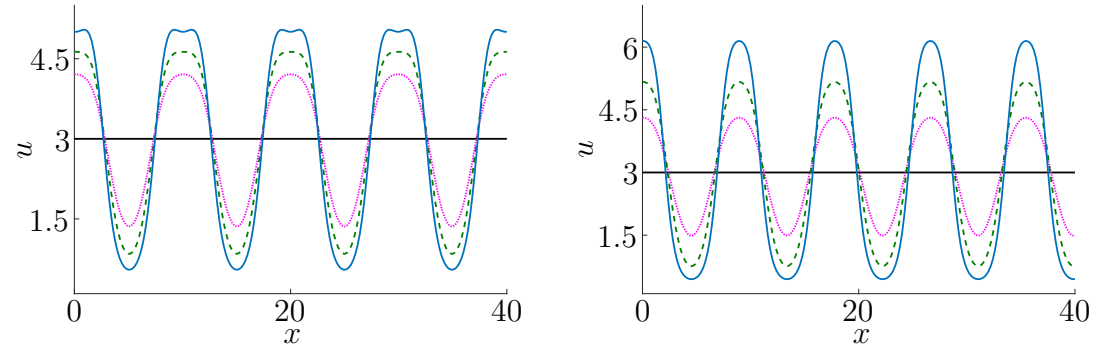

Fig 3. Variations of 4-peak and 4.5-peak patterns for different D_u values

As the coefficient D_u decreases, the wave extrema retreat from the equilibrium value $\bar{u} = 3$. As it gets closer to the bifurcation point $D_u^* = 4.(4)$, the extrema become closer to $\bar{u}$ and converge at D_u^*.

Furthermore, each pattern can be generated in a certain corresponding span of D_u. Such parametric zones, in which the said pattern is preserved by the system, are called structural stability intervals. For some structures these intervals are wide, while for others they can be rather narrow. Outside its interval, the pattern dissipates with time, and a more stable heterogeneous state is observed. Figure 4 displays stability intervals for 4-peak and 4.5-peak patterns. These two types of patterns have the longest structural stability intervals.

The next step is to investigate temporal dynamics. The following color diagrams display the process that takes place: the horizontal axis is the temporal axis, while the vertical one is the spatial axis. The value of u at the given point of space and moment of time is presented by color. Formula (1.4) is used for generating initial conditions, while the scheme (1.3) is used for process modeling of dynamics (see Fig. 5). Below the color diagram, we show snapshots of the system state taken at different moments of time.

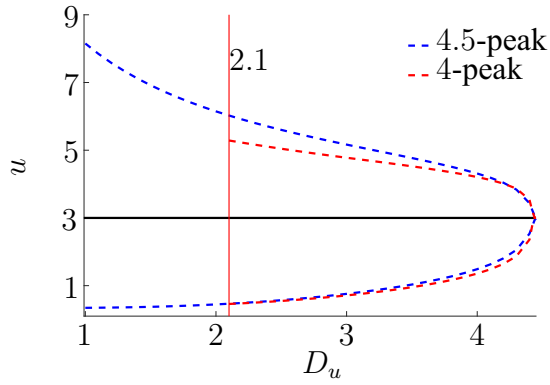

Fig 4. Extrema of patterns in corresponding stability intervals.

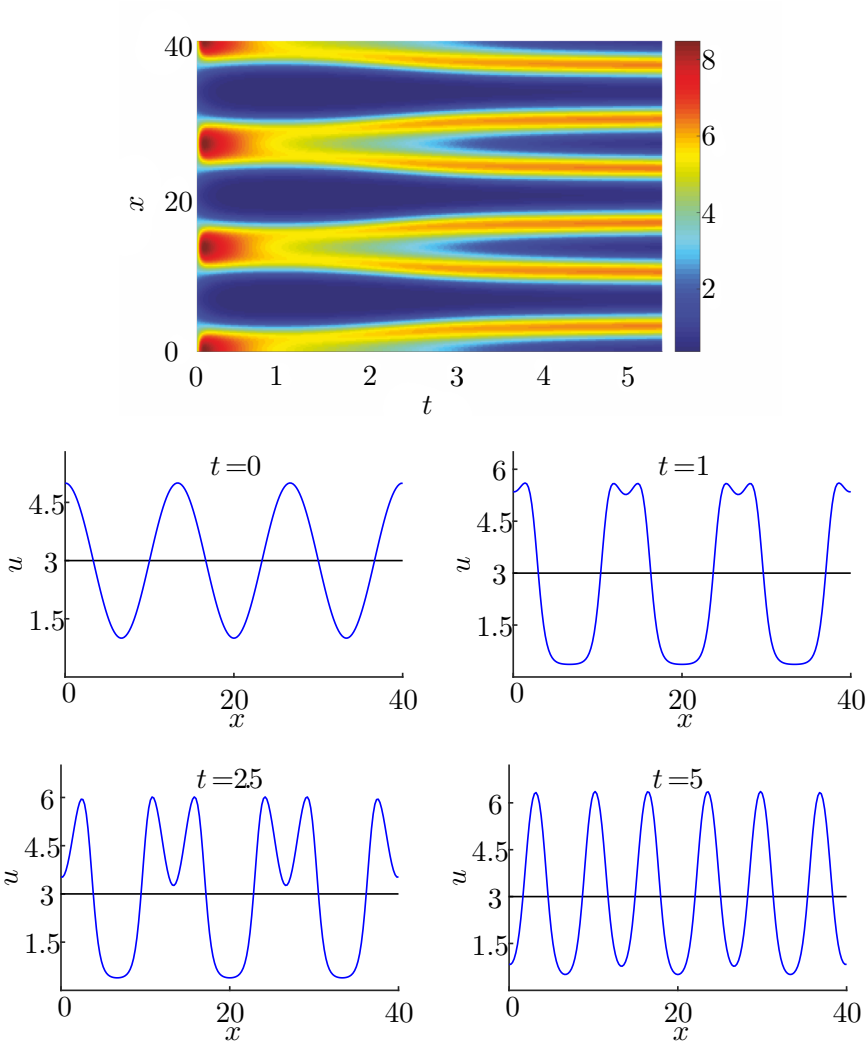

Fig 5. Pattern formation dynamics for $D_u = 2$, $\lambda = 3$, $\varepsilon = 2$

This figure shows the most common pattern formation process. Note that the transition from the initial values to a stable pattern occurs relatively fast in one stage. This, however, is not always the case due to the multistability and coexistence of several patterns. Transient structures may appear during the multi-stage formation process as it is shown in Fig. 6.

The 8-peak and 7-peak patterns can be generated for lower D_u values, however, for $D_u = 2$ these patterns can only appear as transient and are replaced by other, more stable patterns.

Note that such a visualization does not provide sufficient information about less prominent coexisting

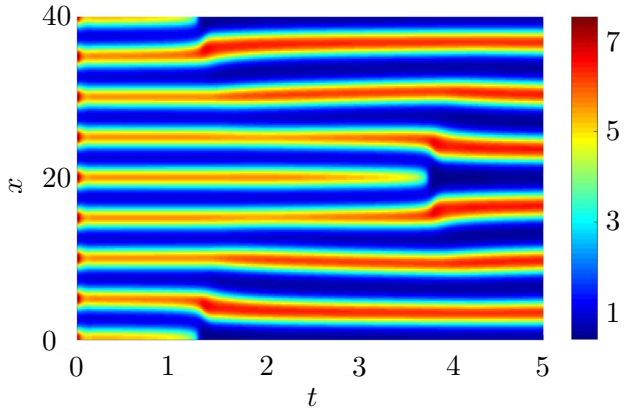

Fig 6. Pattern formation dynamics for $D_u = 2$, $\lambda = 8$, $\varepsilon = 2$

patterns. For further study, the *spatial modality analysis* is applied. In this analysis, we have used the functions $C_k(t)$:

$$C_k(t_j) = C_k^j = \sum_{i=0}^{L_h} h u_{j,i} \cos\left(\frac{2\pi k x_i}{L}\right), \tag{1.5}$$

$$L_h = \frac{L}{h}, \quad x_i = ih, \quad h = 0.2.$$

These functions provide more precise quantitative information on the transient spatial modality of the currently formed patterns. Here, the parameter k corresponds to the quantity of peaks in the pattern. Its values can be integers or half-integers due to the boundary conditions (1.2). The structure with the highest absolute value of C_k will be called dominant. Figure 7 shows results of the spatial modality analysis for the transient process shown in Fig. 6.

At the start of the simulation, the 8-peak pattern is the most prominent, while other kinds of structures appear slowly. Afterwards, the initial pattern is no longer dominant, as the absolute value of C_7 becomes greater than C_8 and the 7-peak pattern is now observed. Finally, at the end of the simulation, C_7 loses its dominance with respect to C_6, which corresponds to the 6-peak pattern seen at the end of Fig. 6. Functions C_k representing the transient patterns will gradually approach zero, while those of the stable structures will remain at fixed values.

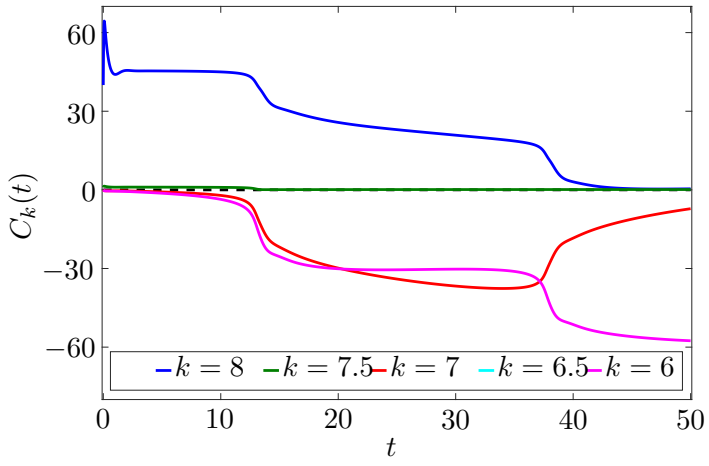

Fig 7. Spatial modality analysis of pattern formation for $D_u = 2$, $\lambda = 8$, $\varepsilon = 2$

§ 2. Stochastic pattern formation

The main focus of this part is studying various stochastic phenomena in the system due to small random perturbations. Adding noise to the model makes it more similar to real processes from nature. The goal is to make predictions for the behavior of such systems. The two noise-induced phenomena viewed in this section are the pattern formation in the Turing stability zone and the transitions between coexisting patterns.

Let us assume $a = 3$, $b = 9$, $D_v = 10$, $D_u = 4.46 > D_u^* = 4.(4)$. For this set of parameters, the deterministic system exhibits the stable homogeneous equilibrium. This equilibrium is used as an initial condition. The system is in the parametric zone of Turing stability, where the pattern generation is impossible if $\gamma = 0$. Adding small random perturbations causes the emergence of states similar to the patterns observed in the previous section. These structures are by no means stable due to the stochastic nature of the model. Simulation results are shown in Fig. 8.

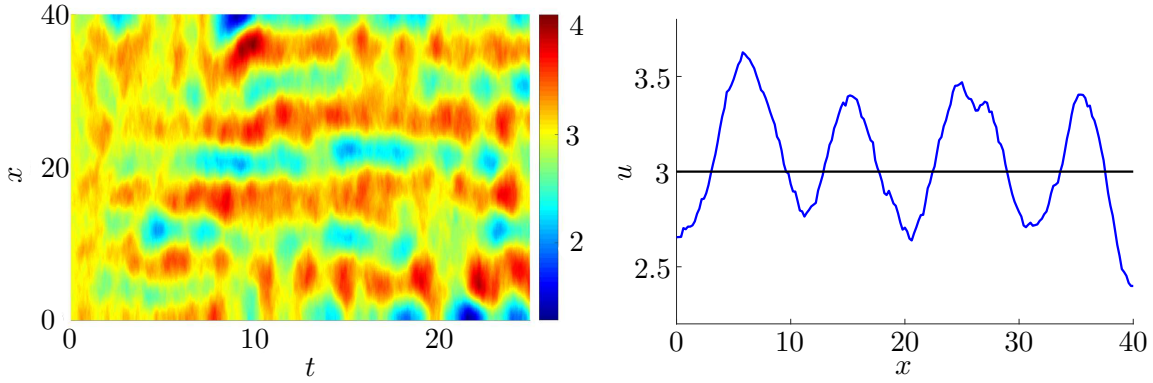

Fig 8. Noise-induced pattern formation $a = 3$, $b = 9$, $D_v = 10$, $D_u = 4.46$, $\gamma = 0.001$: temporal dynamics (left) and state snapshot at $t = 13$ (right)

Despite being in the stability zone, the system with random perturbations is able to generate spatial patterns. Moreover, the system shows multistability: in Fig. 8 two patterns with 4- and 4.5 peaks are prominent. Two matters require investigation: whether or not these are the only possible patterns and which patterns are seen more often than others. For further study, the spatial modality analysis is used. Using the method from the previous section (see formula (1.5)) yields the results displayed in Fig. 9. Here, the dynamics of the coefficients $C_k(t)$ is shown for different k.

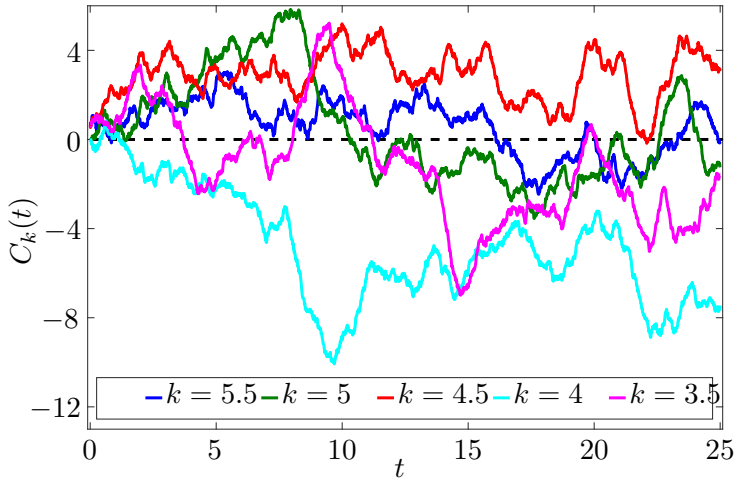

Fig 9. Spatial modality analysis of pattern formation for $a = 3$, $b = 9$, $D_v = 10$, $D_u = 4.46$, $\gamma = 0.001$

These results correlate with the dynamics from Figure 8, but unlike in the deterministic case these curves are difficult to perceive: all modes need to be analyzed, while some of them fluctuate widely. Under these circumstances, another characteristics of the modality are necessary. To estimate the comparative contribution of the spatial mode with k peaks in the time interval $[0, T]$, we will use the *power of kth mode* W_k as follows:

$$W_k = \frac{\tau}{2T} \sum_{j=1}^{T_\tau} \Big(C_k^2(t_{j+1}) + C_k^2(t_j) \Big),$$
$$T_\tau = \frac{T}{\tau}, \quad t_j = j\tau, \quad \tau = 10^{-4}.$$

A calculation of this value provides information on the presence of the mixture of various patterns. A high value of W_k corresponds to the higher weight of k-peak mode with the prolonged period of dominance. Table 1 shows the most notable powers for the simulation described in Fig. 8, where $T = 25$.

Table 1. Mode powers for $D_u = 4.46$, $\gamma = 0.001$

k	3	3.5	4	4.5	5	5.5	6
W_k	0.0344	0.0782	0.2973	0.0948	0.0568	0.0181	0.0079

It can be seen that the 4-peak pattern was the most prominent during the simulation. This is also reflected by the mode powers: W_4 has the greatest value. Using this approach, it is possible to perform a quantitative statistical analysis of the noise-induced pattern formation. Based on these results it is possible to predict (to a certain degree) which pattern will be observed more often than others. In Table 2, mean values gathered from 20 samples are shown. The stochastic nature of the process implies that each time the result is different. However, one can point out the apparent dominance of 3.5-, 4- and 4.5-peak patterns.

Table 2. Mean values of powers for $D_u = 4.46$, $\gamma = 0.001$

k	3	3.5	4	4.5	5	5.5	6
W_k	0.0419	0.1197	0.2118	0.1216	0.0393	0.0221	0.0087

We can summarize that the deterministic model under consideration is multistable and various transient patterns are observed. Due to these factors, the small perturbations can affect the formation dynamics. As a result, the stochastic system generates a different pattern from the one observed in the deterministic model.

Besides the effect on formation dynamics, even weak noise can cause some of the patterns to become unstable and dissipate, while others remain stable. This observation implies difference in the stochastic sensitivity of different coexisting patterns.

Figure 10 shows transition from a stable 7-peak pattern that is generated and preserved by the deterministic model. Applying low intensity noise causes it to dissipate, forming a transient 6-peak pattern, which dissipates as well. At the end of this simulation a relatively stable 5-peak pattern is generated.

This process can be investigated by mode analysis. Figure 11 shows the slow decay of the 7th mode, the temporary emergence of the 6th and the establishment of the 5th mode.

While not yielding much new information that allows prediction of transition dynamics, this technique shows these processes from a new perspective. Furthermore, it can be used for an in-depth study of pattern sensitivity by analyzing fluctuations of corresponding mode and their correlation with noise intensity.

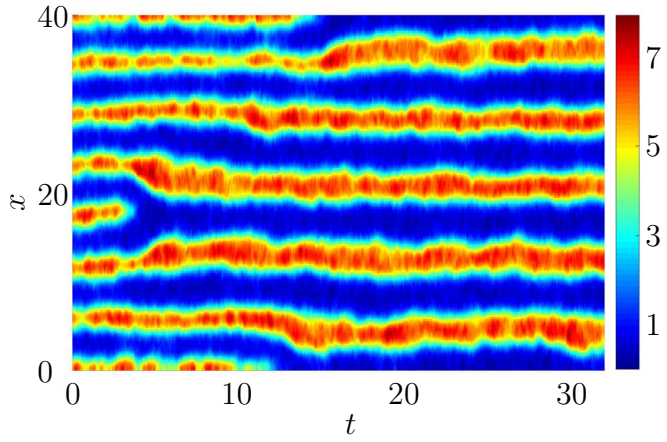

Fig 10. Pattern transitions for $a = 3$, $b = 9$, $D_v = 10$, $D_u = 2$, $\gamma = 0.004$

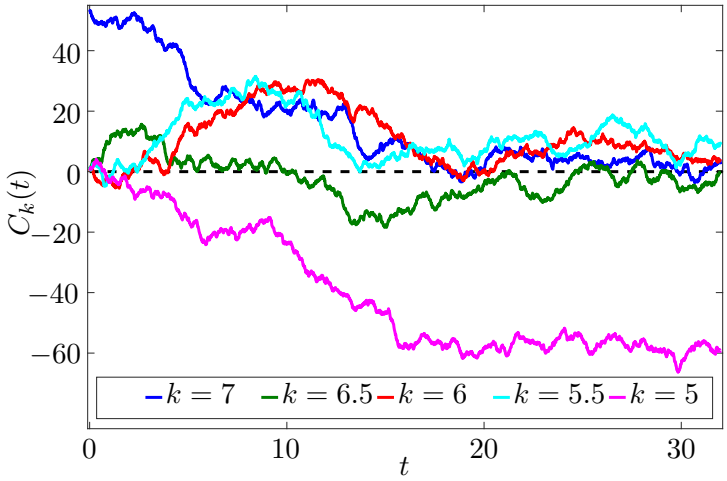

Fig 11. Modality analysis of pattern transitions $a = 3$, $b = 9$, $D_v = 10$, $D_u = 2$, $\gamma = 0.004$

Conclusion

This paper has examined the distributed stochastic Brusselator model with diffusion. Under certain conditions the system meets Turing instability requirements and generates spatially nonhomogeneous stable states. Investigation of its behavior in the Turing instability zone without random perturbations shows that the system is multistable and the number of coexisting patterns may be high. Such structures may have different forms, depending on the diffusion flow difference of the reaction components. While some patterns appear to be stable, others can be observed only as transient structures.

To study processes concerning pattern formation dynamics, the mode analysis method has been introduced. It is shown that the data received from this method correlates with the data obtained from deterministic cases. Mode functions and powers provide additional information necessary for the statistical analysis of stochastic phenomena, the major example being particular pattern dominance.

Finally, the effects of random perturbations have been shown. Small intensity noise causes pattern formation in the Turing stability zone, where deterministic formation is impossible. Furthermore, the multistability persists even in this zone, as the coexisting patterns tend to replace each other. In the stability zone stochastic transitions of coexisting patterns are observed. Under the effect of random perturbations some structures dissipate, though they appeared to be stable in the deterministic case, while less sensitive structures form instead. This implies difference in the stochastic sensitivity of these structures. The said stochastic phenomena are studied by using direct modeling with the assistance of mode analysis.

Funding. This research was supported by the Russian Science Foundation (project no. 16–11–10098).

REFERENCES

1. Murray J. *Mathematical biology*, Berlin: Springer-Verlag, 1993.
2. Nicolis G., Prigogine I. *Self-organization in nonequilibrium systems*, New York: Wiley, 1977.
3. Turing A. The chemical basis of morphogenesis, *Philos. Trans. R. Soc. Lond. B*, 1952, vol. 237, issue 641, pp. 37–72. https://doi.org/10.1098/rstb.1952.0012
4. Kolinichenko A., Ryashko L. Analysis of spatiotemporal self-organization in stochastic population model, *AIP Conference Proceedings*, 2018, vol. 2015, 020041. https://doi.org/10.1063/1.5055114
5. Hoshino T., Liu M.-W., Wu K.-A., Chen H.-Y., Tsuruyama T., Komura S. Pattern formation of skin cancers: Effects of cancer proliferation and hydrodynamic interactions, *Physical Review E*, 2019, vol. 99, 032416. https://doi.org/10.1103/PhysRevE.99.032416
6. Morales M.A., Fernandez-Cervantes I., Augustin-Serrano R., Anzo A., Sampedro M.P. Patterns formation in ferrofluids and solid dissolutions using stochastic models with dissipative dynamics, *Eur. Phys. J. B*, 2016, vol. 89, no. 182. https://doi.org/10.1140/epjb/e2016-70344-7
7. Pablo M., Ramirez S.A., Elston T.C. Particle-based simulations of polarity establishment reveal stochastic promotion of Turing pattern formation *PLoS Comput. Biol.*, 2018, vol. 14, no. 3, p. e1006016. https://doi.org/10.1371/journal.pcbi.1006016
8. Zheng Q., Shen J., Pattern formation in the FitzHugh–Nagumo model, *Computers & Mathematics with Applications*, 2015, vol. 70, issue 5, pp. 1082–1097. https://doi.org/10.1016/j.camwa.2015.06.031
9. Ekaterinchuk E., Ryashko L. Stochastic generation of spatial patterns in Brusselator, *AIP Conference Proceedings*, 2016, vol. 1773, 060005. https://doi.org/10.1063/1.4964980

Received 01.04.2019

Kolinichenko Aleksandr Pavlovich, Master Student, Institute of Natural Sciences and Mathematics, Ural Federal University, ul. Lenina, 51, Yekaterinburg, 620075, Russia.
E-mail: kolinichenko.ale@gmail.com

Ryashko Lev Borisovich, Doctor of Physics and Mathematics, Professor, Department of Theoretical and Mathematical Physics, Institute of Natural Sciences and Mathematics, Ural Federal University, ul. Lenina, 51, Yekaterinburg, 620075, Russia.
E-mail: lev.ryashko@urfu.ru

А. П. Колиниченко, Л. Б. Ряшко

Анализ модальности паттернов в системах реакции-диффузии со случайными возмущениями

Цитата: *Известия Института математики и информатики Удмуртского государственного университета*. 2019. Т. 53. С. 73–82.

Ключевые слова: модель реакции-диффузии, неустойчивость по Тьюрингу, самоорганизация, формирование паттерна, индуцированная шумом динамика, модальный анализ.

УДК: 517.958, 544.431.8

DOI: 10.20537/2226-3594-2019-53-07

В работе исследуется распределенная модель брюсселятора с диффузией. Известно, что в этой модели проявляются бифуркации Андронова–Хопфа и Тьюринга. Показано, что в параметрической зоне диффузионной неустойчивости модель генерирует множество устойчивых пространственно неоднородных структур (паттернов). Эта система демонстрирует феномен мультистабильности с разнообразием устойчивых пространственных структур. В то же время каждый паттерн имеет свой уникальный параметрический диапазон, в котором он может наблюдаться. Акцент сделан на анализе стохастических явлений формирования паттерна и переходов, вызванных малыми случайными возмущениями. Стохастические эффекты изучаются с помощью анализа пространственной модальности. Показано, что структуры обладают различной степенью стохастической чувствительности.

Финансирование. Работа выполнена при поддержке РНФ (проект № 16–11–10098).

Поступила в редакцию 01.04.2019

Колиниченко Александр Павлович, студент магистратуры, Институт Естественных Наук и Математики, Уральский Федеральный Университет, 620075, Россия, г. Екатеринбург, ул. Ленина, 51.
E-mail: kolinichenko.ale@gmail.com

Ряшко Лев Борисович, д.ф.-м.н., профессор, кафедра теоретической и математической физики, Институт Естественных Наук и Математики, Уральский Федеральный Университет, 620075, Россия, г. Екатеринбург, ул. Ленина, 51.
E-mail: lev.ryashko@urfu.ru